J. Mol. Biol. (1994) **236**, 1154–1168

Comparative Studies of High Resolution *Z*-DNA Crystal Structures

Part 1: Common Hydration Patterns of Alternating dC-dG

Reinhard V. Gessner

Institute for Clinical Chemistry and Biochemistry
Rudolf Virchow University Hospital, D-1000 Berlin 19, Germany

Gary J. Quigley

Department of Chemistry, Hunter College, New York, NY 10021, U.S.A.

and Martin Egli†

Organic Chemistry Laboratory
ETH Swiss Federal Institute of Technology, CH-8092 Zürich, Switzerland

The water structure in three crystal forms of the left-handed *Z*-DNA hexamer $[d(CGCGCG)]_2$ has been analyzed. Several common motifs have been found in the first hydration shells. On the convex surface, the major groove of the left-handed conformation, water molecules bridge the guanine O-6 keto groups at GpC steps. Cytosine N-4 nitrogens of opposite strands are hydrated by tandem water molecules. At the bottom of the minor groove, a string of water molecules connects the cytosine O-2 keto groups. Across the minor groove guanine N-2 nitrogens are bridged to phosphate oxygens of cytosine and guanine residues by one or two water molecules. In contrast to the very regular geometry of the water structure around the bases, the arrangement of water molecules between phosphate groups appears to be less ordered. However, there is a strong correlation between the inter-phosphate distances and the number of water molecules or ions which link the phosphate groups. In all three structures various ions, such as sodium and magnesium ions, as well as the protonated amino and imino groups of the polycation spermine displace and replace water molecules in the first hydration shell. Nevertheless, the analysis reveals that numerous first hydration shell water molecules in *Z*-DNA crystals can be regarded as part of the DNA structure. Their positions and thermal parameters are generally independent of changes in the local crystallographic environment.

Keywords: DNA hydration; X-ray crystallography; hydrogen bonding; inter-strand water bridging; sequence-dependent hydration

1. Introduction

Among the structures of double-helical nucleic acid fragments determined by X-ray crystallography, those of the left-handed *Z*-DNA hexamers have been studied in particular detail. Crystals of some left-handed hexamers diffract X-rays exceptionally well compared to other crystalline fragments of DNA and RNA. This allows the visualization of many water molecules and ions surrounding the DNA. The DNA hexamer d(CGCGCG) has been crystallized under various conditions. The original *Z*-DNA structure, here referred to as the mixed spermine/magnesium form, was determined with crystals of DNA grown in the presence of both spermine and magnesium ions (Wang *et al.*, 1979; PDB‡ entry 2DCG, NDB entry ZDF001). In this crystal structure, two spermine molecules and one hydrated magnesium complex are found per DNA duplex. Both spermine

† Author to whom all correspondence should be addressed.

‡ Abbreviations used: PDB, Protein Data Bank; NDB, Nucleic Acid Database.

0022-2836/94/091154-15 $08.00/0

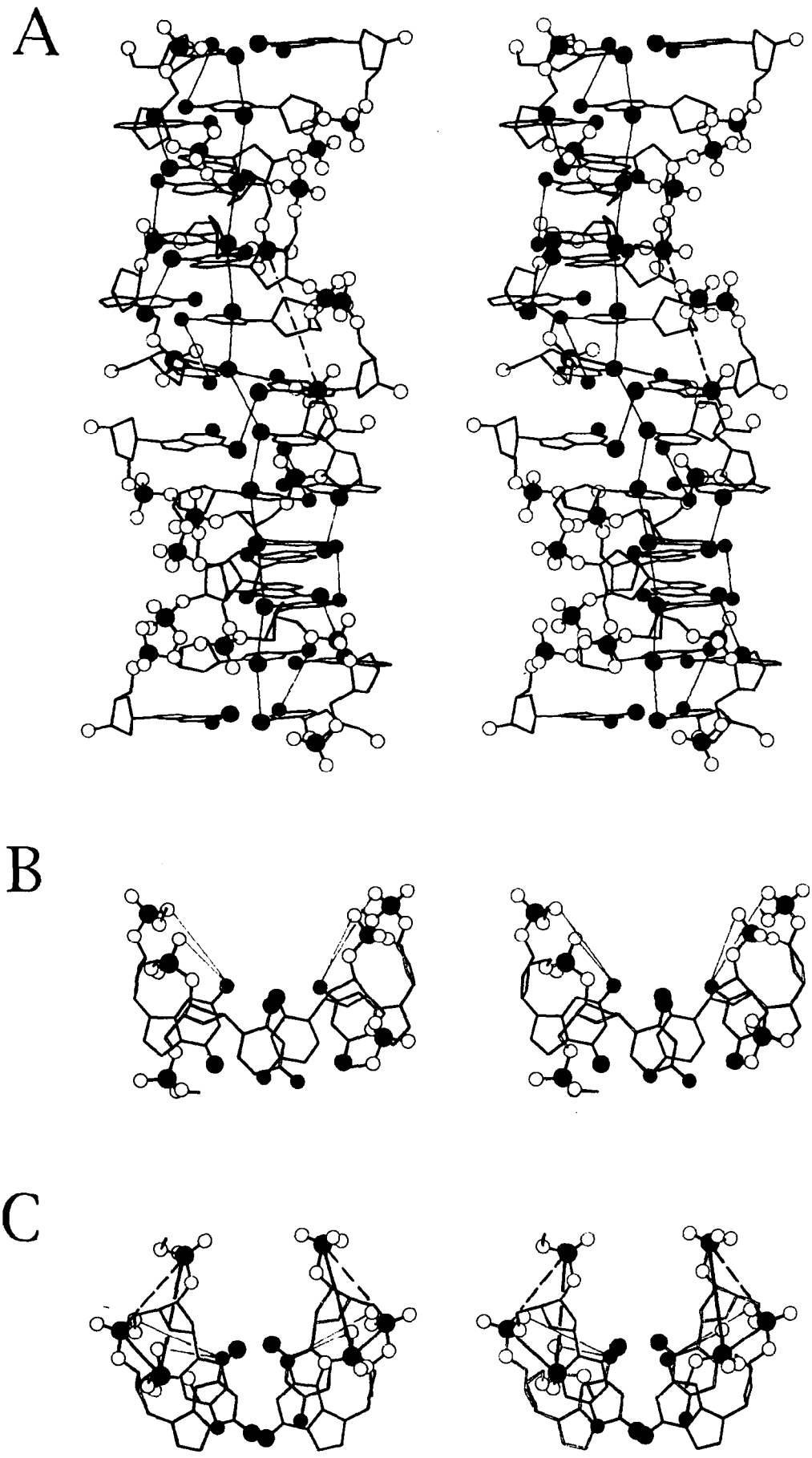

Fig. 1.

molecules bind only in the major groove and to the phosphate groups but do not enter the minor groove. A second, isomorphous crystal structure of the same left-handed hexamer was obtained from crystals grown without spermine in the presence of high concentrations of magnesium ions (Gessner *et al.*, 1985, 1989; PDB entry 1DCG, NDB entry ZDF002). In this magnesium form of d(CGCGCG), four hydrated magnesium ions are surrounding the DNA and give rise to a different solvent structure within the same lattice. Similar to the spermine ions, all four magnesium hexahydrate complexes bind simultaneously to more than one DNA helix, and thereby stabilize the packing. When grown in the absence of any divalent metal cations, but in the presence of spermine, the same DNA hexamer adopts a different orientation in the crystal lattice, resulting in the first of more than a dozen *Z*-DNA hexamer crystal structures that is not isomorphous to the original one (Egli *et al.*, 1991 (room temperature structure); PDB entry 1D18, NDB entry ZDF029; Bancroft *et al.*, 1993 (low temperature structure); PDB entry 131D, NDB entry ZDF035). In this pure-spermine form, one spermine molecule, the inter-helical spermine, binds to three different parallel DNA helices, while the other, the intra-helical spermine, is located in the minor groove, forming hydrogen bonds to two stacked DNA hexamers. In addition, two hydrated sodium ions per DNA duplex were found in the low-temperature structure of that form, the one that will be used for the present analysis of hydration. These three forms of d(CGCGCG) are the most detailed structures of all left-handed hexamers, having been determined at resolutions of 1 Å or better.

The *Z*-DNA double helix is slightly slimmer than the right-handed *A* and *B*-helices and has the appearance of an almost perfectly cylindrical rod (Figure 1A). The major groove of the right-handed conformations is converted into a convex surface in *Z*-DNA, exposing the outer side of the base-pairs directly to the solvent. In contrast, the minor groove is very narrow and deep and extends almost to the helical axis (Figure 1B and C). Left-handed *Z*-DNA is characterized by an alternating conformation of successive base-pairs. Thus, in contrast to *A* and *B*-DNA, two stacked base-pairs constitute the helical repeat. The orientation of the bases relative to the ribose moiety alternates between the *syn* and the *anti* conformation, resulting in a small helical twist (9°, $\sigma = 2°$) and an increased helical rise (4·0 Å, $\sigma = 0{\cdot}3$ Å) at the d(CpG)-step (Figure 1B), and a large helical twist (51°, $\sigma = 2°$) and a decreased helical rise (3·5 Å, $\sigma = 0{\cdot}4$ Å) at the d(GpC)-step (Figure 1C). Other helical parameters, like roll, tilt, propeller twist, buckle and displacement show no significant systematic variation. The alternating *syn/anti* orientation of the N-glycosidic bond in *Z*-DNA is correlated with significant alterations of the ribose pucker and the backbone torsion angles, including the phosphate groups. The smooth ribbon of phosphate groups lining the major groove in *A* and *B*-DNA is thus transformed into the *Z*-DNA-typical zig-zag pattern framing the minor groove (Figure 1A). In the lattices of the three *Z*-DNA hexamers, helices are stacked upon each other along a crystallographic twofold screw axis. This generates an infinite *Z*-DNA helix, which is only interrupted by the lack of phosphodiester bonds between stacked helices every sixth base-pair (Figure 1A).

The structural characteristics of water surrounding nucleic acids have been reviewed in a number of articles (Saenger, 1987; Westhof, 1987, 1988; Berman, 1991, Schneider *et al.*, 1992*a*). Hydration around specific sequences of DNA has been investigated in crystal structures of oligonucleotides in the *A*-DNA (Kennard *et al.*, 1986; Eisenstein *et al.*, 1990), the *B*-DNA (Drew & Dickerson, 1981; Kopka *et al.*, 1983; Cruse *et al.*, 1986; Privé *et al.*, 1987), and the *Z*-DNA conformation (Chevrier *et al.*, 1986; Zhou & Ho, 1990; Schneider *et al.*, 1992*b*). Aspects of the interrelationship between hydration and conformation of nucleic acids have been discussed both on the basis of single crystal structures (Saenger *et al.*, 1986; Shakked *et al.*, 1989; Kagawa *et al.*, 1989) and fiber structures (Harmouchi *et al.*, 1990). The hydration of *B*-DNA has also been simulated with computer calculations (Finney *et al.*, 1985; Subramanian *et al.*, 1988, 1990; Eisenhaber *et al.*, 1990*a*,*b*; Chuprina *et al.*, 1991; Subramanian & Beveridge, 1993).

Here, we report details of the water structure in three crystal structures of left-handed *Z*-DNA

Figure 1. Stereo drawings of $[d(CGCGCG)]_2$ in the pure-spermine form of left-handed *Z*-DNA. A, Two stacked (3′-5′/5′-3′) hexamer duplexes, generating an infinite helix with continuous grooves. DNA hydrogen bond acceptor and donor atoms participating in the groove hydrogen bonding networks are highlighted in color. In the convex surface, guanine O-6 oxygens are red, and cytosine N-4 nitrogens are blue. In the minor groove, cytosine O-2 oxygens are pink, and guanine N-2 nitrogens are light blue. Phosphorus atoms are black. Lines connecting the functional groups in matching colors indicate the longitudinal water bridges in the grooves. The continuous and broken orange lines connecting phosphorus atoms from 2 duplexes across the minor groove represent distances which are referred to as types 4 and 5, respectively, in the analysis of phosphate hydration. B, d(CpG)-step, C, d(GpC)-step. The projections are roughly along the perpendicular to the top base-pair (filled bonds), and show base-pairs C(3)·G(10) and G(4)·C(9) (below, open bonds), as well as base-pairs G(2)·C(11) and C(3)·G(10) (below, open bonds). O3′ and O5′ of adjacent residues have been included to allow differentiation between bridging and non-bridging phosphate ester oxygens. Color coding is identical to A, and light blue lines indicate the transversal water bridges between N-2 nitrogens and phosphate groups in the minor groove. The continuous and broken green lines connecting consecutive intra-strand phosphorus atoms in C represent distances which are referred to as types 1 and 2, respectively, in the analysis of phosphate hydration. Similarly, brown lines represent type 3 distances.

hexamers with the sequence d(CGCGCG). Several aspects distinguish the analyzed structures from others of right and left-handed DNA fragments of which hydration was studied. (1) All three structures were determined at a resolution of 1 Å, considerably higher than those reported for any other oligonucleotide structure. (2) Crystallographic data were recorded either at 10°C or at low-temperature (−110°C), allowing to assess the effect of temperature on the solvent structure. (3) In the three structures the same DNA hexamer is surrounded by different ionic environments. This enables one to study the impact of different counter ions on DNA hydration. (4) Among the included crystal structures, two distinct lattices exist. Thus, the impact of crystal packing on the hydration pattern can be analyzed. A careful examination of the first-shell water and ion structure in the three crystal forms should allow us to distinguish between systematic preserved hydration patterns around the duplex, and those which are introduced by ion interactions or packings of duplexes. It is interesting to look for such shared hydration patterns because common hydration motifs which are found in spite of the above non-ideal conditions are likely to be also present in solution, where interactions between DNA molecules are negligable and ion interactions are more dynamic. Such an analysis should also provide an answer to the question whether the intrinsic symmetry of left-handed *Z*-DNA is reflected in the water structure. This is of particular interest in the view of the possible elucidation of principles for the hydration of DNA in general.

2. Methods

(a) *Structure determination and refinement.*

Crystallization, structure solution and refinement for the 3 forms were reported previously (Wang *et al.*, 1979; Gessner *et al.*, 1985, 1989; Egli *et al.*, 1991; Bancroft *et al.*, 1993). Crystallization conditions, crystal data, as well as parameters for data collection and refinement are listed in Table 1. All 3 structures were refined using the Konnert–Hendrickson least-squares procedure (Hendrickson & Konnert, 1981), as modified for nucleic acids (Quigley *et al.*, 1978). In general, the error rate of the assignment of water molecule positions strongly correlates with the resolution and quality of the crystallographic data, and with the distance from well-defined hydrogen bond acceptor and donor groups of the DNA. Higher resolution allows the accurate assignment of more water molecule positions, whereas limited resolution can lead to difficulties in the distinction between solvent positions and electron density noise. Occasionally, water positions did not refine well and most of the density at their assumed locations was lost during subsequent refinement cycles. This can be interpreted by partial occupancies of these positions. In regions further away from the DNA, multiple water structures seem to exist, rendering any attempt impossible to refine specific solvent positions. The often string-like electron density in such areas may

Table 1

Crystallization conditions, crystal data, and data collection and refinement parameters for the three crystal forms of d(CGCGCG)

Parameter	Mixed spermine/ magnesium form	Magnesium form	Pure-spermine form
Crystallization conditions	2 mM DNA 10 mM spermine·4HCl 15 mM $MgCl_2$ 30 mM Na cacodylate (pH 7) 5% isopropanol	1·4 mM DNA 120 mM $MgCl_2$ 20 mM Na cacodylate (pH 7) 10% MPD	1·4 mM DNA 15 mM spermine·4HCl 20 mM Na cacodylate (pH 7) 20% MPD
Crystal size (mm)	0·7 × 0·7 × 0·5	0·7 × 0·3 × 0·3	0·35 × 0·3 × 0·3
Unit cell dimensions (Å)	a = 17·88 b = 31·55 c = 44·58	a = 18·01 b = 31·03 c = 44·80	a = 18·27 b = 30·69 c = 42·46
Cell volume (Å^3)	25,148	25,036	23,808
Space group	$P2_12_12_1$	$P2_12_12_1$	$P2_12_12_1$
Scan method	ω	ω	ω
Temperature (°C)	10	10	−110
Resolution (Å)	0·9	1·0	1·0
Reflections above 2σ level	15,000	10,893	9691
Solution method	Multiple isomorphous replacement	Molecular replacement	Translation/rotation function
Final R-factor (%)	14	17·5	18·0
Number of atoms in the asymmetric unit	DNA: 240 spermine: 28 Mg ions: 1 waters: 74	DNA: 240 Mg ions: 4 waters: 85	DNA: 240 spermine: 28 Na ions: 2 waters: 62
ρcalc (g/cm^3)	1·41	1·37	1·43
ρexp (g/cm^3)	1·49	—	—
r.m.s. deviations from ideal bond lengths (Å)	—	0·04	0·03

represent an array of partially occupied positions. In addition, phosphate groups are often characterized by high temperature factors and can sometimes exist in multiple conformations that can be refined individually (Wang *et al.*, 1981; Egli *et al.*, 1991, Chen & Quigley, 1992). In the case of the 3 reported structures, water positions were never restrained with respect to the DNA. Spermine molecules and ion complexes were only restrained intra-molecularly.

(b) *Water content of Z-DNA crystals*

Densities were calculated from crystallographic data for the 3 structures, and for the mixed spermine/magnesium form, the density was in addition measured by the floating method (CCl_4/*o*-xylene gradient). The calculated densities of the 3 d(CGCGCG) crystals described here are quite similar (Table 1). Differences between the calculated densities are not only caused by slight alterations of the packing due to the presence of different ions in the 3 forms, but also reflect differences in solvent refinement that depend on the respective resolution limits. The small unit cell volume of the pure-spermine form crystal is only partly the result of the low-temperature measurement. At room temperature it is 24.437 $Å^3$ (Egli *et al.*, 1991), and thus 2·8% smaller than the one of the mixed spermine/magnesium form, and 2·4% smaller than the one of the magnesium form. The ordered water contents (w/w; including only crystallographically refined water molecules; M_r d(CGCGCG) (single strand) = 1788·18 g) for the 3 crystals are 25% (mixed spermine/magnesium form), 29% (magnesium form) and 21% (pure-spermine form). The measured density of the mixed spermine/magnesium form crystals is 1·49 g/cm^3. The difference between measured and calculated densities with the latter form would account for another 16 water molecules per asymmetric unit, indicating that more than 80% of the water positions were determined. We can speculate that most of these missing water molecules form part of the second and higher hydration spheres and are therefore less important for an analysis of structural motifs in the first hydration sphere of DNA.

(c) *Analysis of water structure*

A close inspection of the chemical and geometric properties of *Z*-DNA reveals that only a limited number of atoms are able to form hydrogen bonds to water molecules. Only these were consequently considered in the present work (see highlighted atoms in Figure 1). Bridges between functional groups on the surface of DNA can be formed by either 1, 2 or more water molecules. Due to the rapidly growing number of involved water molecules and the even larger number of alternative bridges, a reasonable description of conserved hydration motifs becomes unfeasible. In addition, we can assume that only mono- and dimolecular water bridges contribute effectively to conformational stabilization in DNA. Only these 2 classes of water bridges have therefore been included in the present analysis.

3. Results and Discussion

(a) *Water structure on the convex surface*

Although several different cations coordinate to the convex base surface of the *Z*-DNA helix, two common water structure motifs are consistently found in the three crystal structures. The bridges connecting the cytosine N-4 amino groups are shown schematically in Figure 2. The regular pattern of hydrogen bond distances and angles as well as the low temperature factors of solvent molecules indicate a particularly stable water structure. Even the close proximity of two hydrated magnesium ions at residues C3 and C9 in the magnesium form does not have any influence on the geometry. Another water structure motif on the convex surface is shown schematically in Figure 3. This motif involves a direct water bridge between the guanine O-6 keto groups at GpC steps from opposite strands. The geometry, including the hydrogen bond angle of less than 80°, is very similar to that of the cytosine O-2 water chain (see section (b) below). However, the large base-pair shear separates the keto groups in the CpG step by more than 5 Å and renders a continuous water chain impossible (Figure 1A and B). It is not surprising that the hydration of the O-6 oxygens on the convex surface is somewhat less regular than that of the N-4 nitrogens, since cations such as spermine or hydrated magnesium ions, in addition to interacting with phosphate groups, coordinate preferably to acceptors O-6 and N-7 of guanine on the convex surface. In the mixed spermine/magnesium form, an imino nitrogen of a coordinated spermine molecule bridges two O-6 oxygens (Figure 3, left). Its methylene carbon atoms displace the water molecule from the O-6 oxygens of the next dinucleotide repeat. In the magnesium form, the O-6 oxygens from stacked terminal guanine residues are bridged by two ligand water molecules from a magnesium ion cluster (Figure 3, center). Both conserved hydration patterns on the convex surface are thus longitudinal arrangements. Although several water-mediated hydrogen bonds between base atoms and phosphate groups more or less within the plane of the base-pair occur in *Z*-DNA as well, these longitudinal solvent bridges render the hydration of the outer surface of the left-handed duplex quite different from the hydration of the topological equivalent in *B*-DNA. For both types of water bridges on the convex suface, the hydrogen bond angles at water molecules are consistently smaller than expected.

(b) *Water structure in the minor groove*

Near the bottom of the minor groove a string of water molecules systematically bridges the O-2 keto groups of the cytosine residues from alternating strands (Figure 4). In the pure-spermine form, a spermine molecule binds in the minor groove of the *Z*-DNA hexamer and contacts its floor *via* the two central imino nitrogens (Figure 4, right). These are hydrogen-bonded to O-2 oxygens of cytosines C1* (symmetry-related) and C7 as well as cytosines C5 and C9, and replace two water molecules from the minor groove hydration spine. The neighboring methylene groups of the spermine displace two further water molecules. The hydrogen bond angles of water molecules are consistently lower than

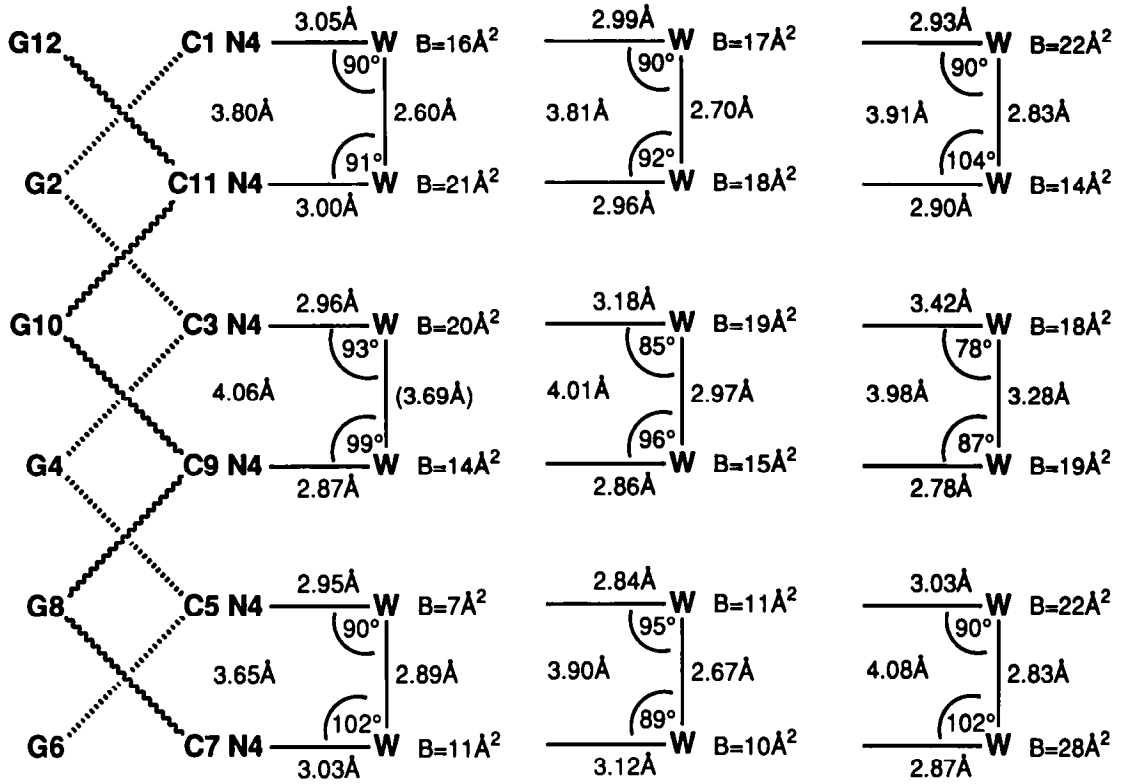

Figure 2. Schematic diagram of the water structure bridging cytosine N-4 groups on the convex surface in the mixed spermine/magnesium form (left), the magnesium form (center), and the pure-spermine form (right). Connectivites of the oligonucleotide chains are indicated by dotted (C1 to G6) and wavy lines (C7 to G12). Numbers next to N-4 atoms represent distances between them. Hydrogen bonds are continuous lines with distances next to them, and bond angles at water molecules (W) as well as their isotropic temperature factors are listed.

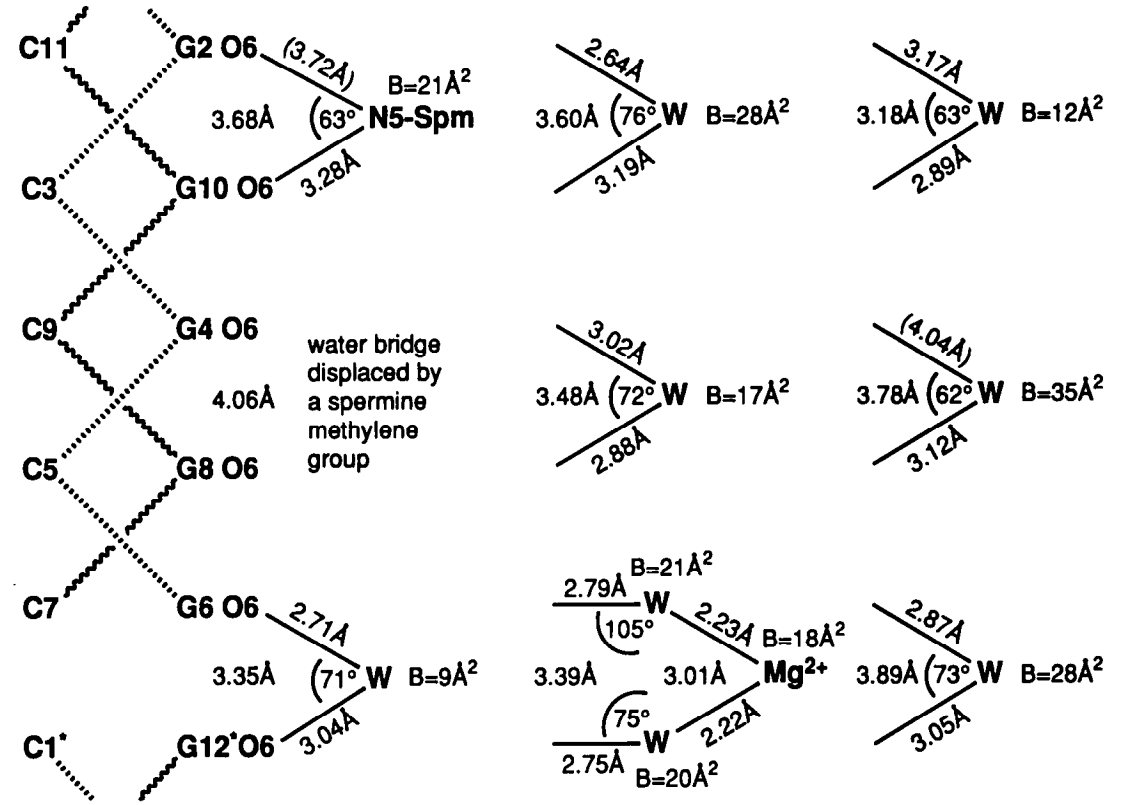

Figure 3. Schematic diagram of the water structure bridging guanine O-6 groups on the convex surface in the mixed spermine/magnesium form (left), the magnesium form (center), and the pure-spermine form (right). Asterisks designate symmetry-related residues and Spm is spermine. For other symbols see the legend to Figure 2.

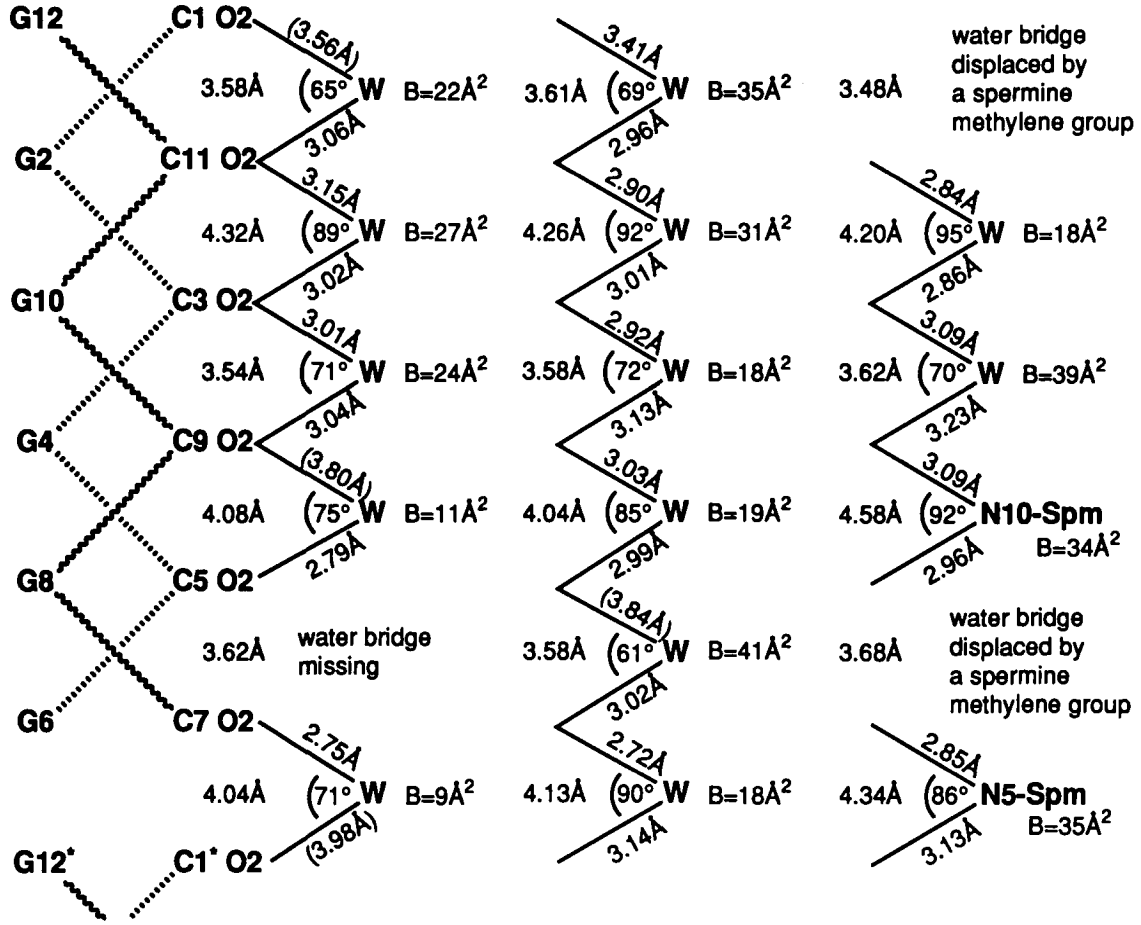

Figure 4. Schematic diagram of the water structure bridging cytosine O-2 groups in the minor groove in the mixed spermine/magnesium form (left), the magnesium form (center), and the pure-spermine form (right). For symbols see the legends to Figures 2 and 3.

expected for an ideal sp^3 hybrid. However, the low temperature factors of some of these water molecules indicate a stable coordination. Since both hydrogen atoms of the water molecules are involved in the bonding to the keto groups, one can expect an increased polarization and repulsion of the lone pair electrons which would contribute to the stabilization of a smaller bonding angle.

Both other hydrogen bonding patterns in the minor groove are oriented within the plane of the bases rather than parallel to the helix axis, and involve water bridges between the guanosine N-2 amino group and the 3′ and 5′-phosphate oxygens (Figures 1B, 1C, 5 and 6). The water structure to the 3′-phosphate oxygens is even found when no phosphodiester is present, as in the case of the terminal guanosine residues G6 and G12 in the mixed spermine/magnesium and magnesium forms (Figure 5). There, the water bridges end at the terminal 5′-hydroxyl group of the next stacked helix instead. Due to the altered relative orientations of duplexes in the pure-spermine form, the water bridges end at the phosphate oxygen atoms of adjacent duplexes in that structure (Figure 5).

Z_I and Z_{II} are alternative conformations adopted by the backbone of left-handed *Z*-DNA (Wang *et al.*, 1981; Egli *et al.*, 1991; Chen & Quigley, 1992). In the Z_{II} backbone the phosphate group is rotated towards the convex surface, away from the minor groove. This results in longer distances between the N-2 amino group and the phosphate oxygen atoms in the minor groove. In the magnesium and mixed spermine/magnesium forms, the Z_{II} conformation of phosphate P5 interrupts the water bridge to guanosine G4. In the magnesium form, this alteration also disrupts the water bridge between guanosine G4 and its 5′-phosphate group (Figure 6). Similar to residue C5 in the two other forms, the backbone around phosphate P9 in the pure-spermine form adopts a partial Z_{II} conformation, and the transversal water bridge to guanosine G8 is therefore missing (Figure 5). Compared to most of the transversal bridges involving two water molecules, those directly bridging N-2 nitrogens and 3′-phosphates at residues G2 and G10 (for the mixed spermine/magnesium form also residue G8) have very low temperature factors indicating stable hydrations (Figure 5).

The second transversal water bridges in the minor groove from guanosine N-2 to the 5′-phosphate oxygen share the first water molecule with the other water bridge. This pattern then branches off and forms hydrogen bonds through other solvent molecules to the 5′-phosphate group. At residue G8

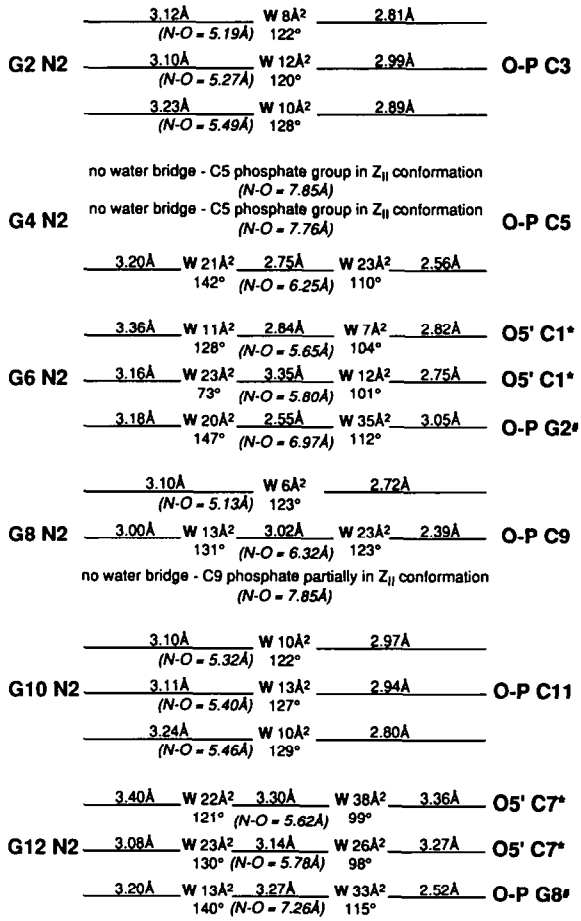

Figure 5. Schematic diagram of the water structure bridging guanine N-2 amino groups to the minor groove oxygen of the 3'-phosphate group (formally assigned to the next residue) in the minor groove in the mixed spermine/magnesium form (top lines), the magnesium form (middle lines), and the pure-spermine form (bottom lines). Residues from symmetry-related duplexes are marked with asterisks (stacked duplexes) or # (parallel duplexes).

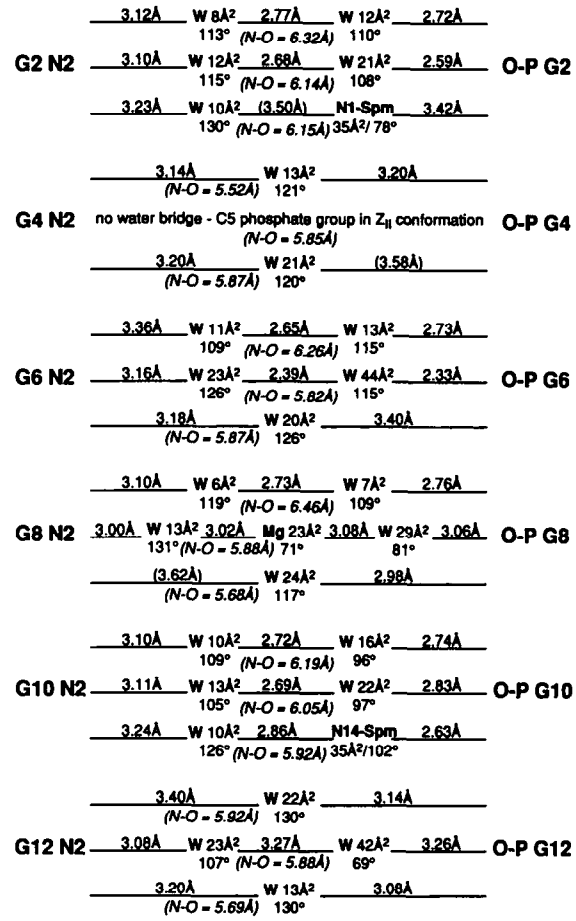

Figure 6. Schematic diagram of the transverse water structure bridging guanine N-2 amino groups to the 5'-phosphate group of the same nucleotide in the minor groove in the 3 forms. For symbols see the legend to Figure 5.

in the magnesium form the second water molecule is substituted by a magnesium ion (Figure 6). In the pure-spermine form, the minor groove spermine contacts the floor of that groove only with its central eight atoms, including the two imino nitrogens. The outer methylene chains adopt sharp turns away from the groove and both terminal protonated amino nitrogen atoms contact phosphate oxygen atoms and water molecules from inside the minor groove. Thus, they replace one of the two water molecules between guanosines G2 and G10 and their respective 5'-phosphate groups (Figure 6). As with the transversal bridges from guanosine N-2 to their 3'-phosphate groups, bridges with just one water molecule are usually associated with N···O-P distances of less than 6 Å.

(c) *Intra-strand water structure between anionic phosphate groups*

In order to facilitate the description of phosphate hydration, the closest distances between intra-strand phosphate groups have been classified into three types. Type 1 refers to the 5'-3' phosphate distance in the guanosine residues (Figure 1C, continuous green lines), and type 2 to the corresponding distance in the cytidine residues (Fig. 1C, broken green lines). Type 3 refers to the 5'-3' phosphate distance in the GpC dinucleotide step (Fig. 1C, brown lines). The corresponding distance in the CpG dinucleotide step is considerably larger and the two phosphate groups are also shielded from each other by a deoxyribose moiety at this step. Distances and water structure for all three intra-strand types are listed in Table 2. Only water bridges consisting of up to two water molecules or ions were included.

Type 1 distances are generally linked by two water molecules. The contacts between phosphates framing guanosine 10 are the closest among type 1 distances in the magnesium ion-containing forms. In these two forms, a second bridge between P10 and P11 is formed by a single water molecule. Similarly, P2 and P3 in the pure-spermine form are bridged by a single water molecule. In the mixed spermine/magnesium and magnesium forms, phosphate P5 adopts a Z_{II} conformation, and in the pure-spermine

Table 2

Intra-strand water structure between phosphate groups

Residues	P···P distance	PO···OP distance	Water structure (maximum of 2 bridging water molecules or ion atoms)
A. *Mixed spermine/magnesium form*			
Type 1 distances			
P2···P3	6·37 Å	5·11 Å	P-O···2·72 Å···$W^{12,A^2}_{110^\circ}$···2·77 Å···$W^{8,A^2}_{110^\circ}$···2·81 Å···O-P
			P-O···2·93 Å···$W^{34,A^2}_{115^\circ}$···2·83 Å···$W^{45,A^2}_{85^\circ}$···2·69 Å···O-P
P4···P5*	7·17 Å*	7·42 Å*	None
P8···P9	6·27 Å	4·84 Å	P-O···2·92 Å···$W^{15,A^2}_{135^\circ}$···2·83 Å···$W^{11,A^2}_{108^\circ}$···2·77 Å···O-P
			P-O···2·92 Å···$W^{15,A^2}_{115^\circ}$···3·24 Å···$SpmN1^{5,A^2}_{77^\circ}$···2·87 Å···O-P
P10···P11	6·26 Å	4·66 Å	P-O···2·99 Å···$W^{16,A^2}_{99^\circ}$···3·14 Å···O-P
			P-O···2·74 Å···$W^{16,A^2}_{96^\circ}$···2·72 Å···$W^{10,A^2}_{114^\circ}$···2·97 Å···O-P
Mean	6·30 Å	4·87 Å	
(σ)	(0·06 Å)	(0·23 Å)	
Type 2 distances			
P3···P4	5·90 Å	4·82 Å	P-O···2·69 Å···$W^{45,A^2}_{83^\circ}$···3·08 Å···$W^{25,A^2}_{93^\circ}$···3·14 Å···O-P
			P-O···2·81 Å···$W^{8,A^2}_{102^\circ}$···3·07 Å···$W^{40,A^2}_{106^\circ}$···3·22 Å···O-P
			P-O···2·68 Å···$W^{30,A^2}_{92^\circ}$···2·50 Å···$W^{25,A^2}_{159^\circ}$···3·14 Å···O-P
P5*···P6	6·50 Å*	6·09 Å*	None
P9···P10	6·02 Å	5·07 Å	P-O···2·87 Å···$SpmN1^{5,A^2}_{90^\circ}$···2·78 Å···$W^{7,A^2}_{119^\circ}$···2·65 Å···O-P
P11···P12	5·81 Å	4·66 Å	P-O···2·75 Å···$W^{14,A^2}_{112^\circ}$···2·87 Å···O-P
Mean	5·91 Å	4·85 Å	
(σ)	(0·11 Å)	(0·21 Å)	
Type 3 distances			
P2···P4	10·31 Å	8·61 Å	None
P4···P6	8·77 Å	6·60 Å	P-O···2·46 Å···$W^{28,A^2}_{92^\circ}$···3·19 Å···W^{34,A^2}_{124}···2·68 Å···O-P
			P-O···3·20 Å···$W^{13,A^2}_{84^\circ}$···2·91 Å···$W^{34,A^2}_{131^\circ}$···2·68 Å···O-P
P6···P2†	10·21 Å	8·38 Å	None
P8···P10	10·52 Å	8·73 Å	None
P10···P12	9·91 Å	7·79 Å	None
P12···P8†	9·22 Å	7·08 Å	P-O···3·14 Å···$W^{22,A^2}_{105^\circ}$···3·16 Å···$W^{39,A^2}_{113^\circ}$···3·21 Å···O-P
Mean	9·82 Å	7·87 Å	
(σ)	(0·69 Å)	(0·87 Å)	
B. *Magnesium form*			
Type 1 distances			
P2···P3	6·34 Å	4·98 Å	P-O···2·59 Å···$W^{21,A^2}_{108^\circ}$···2·68 Å···$W^{12,A^2}_{111^\circ}$···2·99 Å···O-P
P4···P5*	7·23 Å*	7·40 Å*	None
P8···P9	6·65 Å	5·15 Å	P-O···3·06 Å···$MgW^{29,A^2}_{81^\circ}$···3·08 Å···$MgW^{29,A^2}_{147^\circ}$···2·39 Å···O-P
P10···P11	6·20 Å	4·66 Å	P-O···2·80 Å···$W^{28,A^2}_{101^\circ}$···3·22 Å···O-P
			P-O···2·80 Å···$W^{22,A^2}_{97^\circ}$···2·69 Å···$W^{13,A^2}_{115^\circ}$···2·94 Å···O-P
Mean	6·40 Å	4·93 Å	
(σ)	(0·23 Å)	(0·25 Å)	
Type 2 distances			
P3···P4	5·79 Å	4·35 Å	P-O···2·81 Å···$W^{32,A^2}_{91^\circ}$···3·26 Å···O-P
			and 6 more bridges each involving 2 water molecules
P5*···P6	6·61 Å*	6·24 Å*	P-O···2·89 Å···$MgW^{10,A^2}_{150^\circ}$···2·63 Å···$MgW^{25,A^2}_{107^\circ}$···2·60 Å···O-P
P9···P10	6·35 Å	5·39 Å	P-O···2·39 Å···$MgW^{23,A^2}_{152^\circ}$···3·10 Å···$MgW^{28,A^2}_{88^\circ}$···2·80 Å···O-P
			P-O···2·39 Å···$MgW^{23,A^2}_{94^\circ}$···2·70 Å···$MgW^{14,A^2}_{98^\circ}$···2·73 Å···O-P
P11···P12	5·65 Å	4·41 Å	P-O···2·72 Å···$W^{20,A^2}_{102^\circ}$···2·95 Å···O-P
			P-O···2·94 Å···$W^{13,A^2}_{108^\circ}$···2·91 Å···$W^{38,A^2}_{97^\circ}$···3·39 Å···O-P
Mean	5·93 Å	4·72 Å	
(σ)	(0·37 Å)	(0·58 Å)	
Type 3 distances			
P2···P4	9·98 Å	8·06 Å	None
P4···P6	9·35 Å	7·28 Å	None
P6···P2†	10·33 Å	8·31 Å	None
P8···P10	9·65 Å	7·72 Å	P-O···3·06 Å···$MgW^{29,A^2}_{133^\circ}$···3·00 Å···$MgW^{28,A^2}_{144^\circ}$···2·80 Å···O-P
P10···P12	9·72 Å	7·72 Å	None
P12···P8†	9·83 Å	7·70 Å	None
Mean	9·81 Å	7·80 Å	
(σ)	(0·33 Å)	(0·35 Å)	

Table 2 *(continued)*

Residues	P···P distance	PO···OP distance	water structure (maximum of 2 bridging water molecules or ion atoms)
C. Pure spermine form			
Type 1 distances			
P2···P3	6·40 Å	4·95 Å	**P-O**···3·47 Å···$W^{22\,A^2}_{101°}$···2·94 Å···**O-P**
P4···P5	6·47 Å	5·20 Å	**P-O**···2·92 Å···$W^{34\,A^2}_{82°}$···3·21 Å···$W^{39\,A^2}_{141°}$···3·17 Å···**O-P**
P8···P9*	6·83 Å*	7·23 Å*	None
P10···P11	6·48 Å	5·06 Å	**P-O**···2·64 Å···**SpmN1**$^{35\,A^2}_{102°}$···2·86 Å···$W^{10\,A^2}_{94°}$···2·79 Å···**O-P**
Mean	6·45 Å	5·07 Å	
(σ)	(0·04 Å)	(0·13 Å)	
Type 2 distances			
P3···P4	6·23 Å	5·26 Å	**P-O**···2·73 Å···$W^{17\,A^2}_{96°}$···2·70 Å···**G6†-O3′**$^{8\,A^2}_{91°}$···2·75 Å···**O-P**
P5···P6	5·71 Å	4·24 Å	**P-O**···2·56 Å···$W^{23\,A^2}_{108°}$···2·69 Å···**O-P**
P9*···P10	6·53 Å*	6·45 Å*	None
P11···P12	5·92 Å	4·79 Å	**P-O**···2·79 Å···$W^{10\,A^2}_{99°}$···2·78 Å···$W^{19\,A^2}_{117°}$···2·61 Å···**O-P**
Mean	5·95 Å	4·76 Å	
(σ)	(0·26 Å)	(0·51 Å)	
Type 3 distances			
P2···P4	10·66 Å	8·86 Å	None
P4···P6	8·76 Å	6·45 Å	**P-O**···3·55 Å···$W^{22\,A^2}_{79°}$···2·71 Å···$W^{23\,A^2}_{95°}$···2·69 Å···**O-P**
P6···P2†	8·30 Å	6·20 Å	**P-O**···2·65 Å···$W^{31\,A^2}_{70°}$···2·86 Å···$W^{33\,A^2}_{126°}$···3·08 Å···**O-P**
P8···P10	8·28 Å	6·03 Å	**P-O**···2·98 Å···$W^{23\,A^2}_{90°}$···2·91 Å···$W^{32\,A^2}_{104°}$···2·68 Å···**O-P**
			P-O···2·85 Å···$W^{35\,A^2}_{126°}$···2·78 Å···$W^{23\,A^2}_{115°}$···2·86 Å···**O-P**
P10···P12	10·16 Å	8·33 Å	None
P12···P8†	8·71 Å	6·46 Å	**P-O**···3·08 Å···$W^{13\,A^2}_{89°}$···3·20 Å···$W^{34\,A^2}_{116°}$···2·54 Å···**O-P**
Mean	9·15 Å	7·06 Å	
(σ)	(1·01 Å)	(1·22 Å)	

The Table lists selected intra-strand distances between phosphorus atoms and the shortest of the 4 possible P-O···O-P distances, as well as distances between phosphate oxygen atoms and water molecules and between water molecules. Angles at the water molecules are in subscript, their isotropic temperature factors are in superscript. Symmetry-related atoms are marked (†), and an asterisk (*) indicates that the phosphate group P5 (P9 in the pure-spermine form) is found in the Z_{II} conformation. The marked inter-phosphate distances are therefore deviating and have not been used to calculate the average distance and its standard deviation. The distance types 1, 2 and 3 are defined in the text.

form, phosphate P9 adopts a partial Z_{II} conformation. The Z_{II} conformation greatly increases type 1 distances between phosphates, disrupting water bridges at such sites (see Table 2).

The amino nitrogen atoms of a spermine molecule in the mixed spermine/magnesium form and one of the magnesium complexes in the magnesium form occupy very similar positions on the DNA surface. They contribute to the bridging of phosphates P8 and P9 in the respective structures. Since two water molecules from the coordination sphere of a magnesium ion can span a larger distance than the primary amino group of spermine, the resulting distances between water molecules and between water molecules and phosphate groups, respectively, in the magnesium form are shorter on average compared to the corresponding distances in the mixed form. The relative orientations of spermine molecules and DNA in the pure-spermine form do not resemble the ones observed in the mixed spermine/magnesium form. In the first form, a spermine molecule is located in the minor groove and one of its amino nitrogen atoms replaces a water molecule in the solvent bridge between phosphates P10 and P11.

Type 2 distances between cytosine phosphate groups are more variable than the type 1 distances. Again, the closest phosphate pairs are bridged by just one water molecule. Although type 2 distances are slightly shorter on average compared to type 1 distances, a Z_{II} conformation of the phosphate group still results in a disruption of the water structure between intra-strand phosphate groups. The only exception is found in the magnesium form, where phosphate P5, which adopts a Z_{II} conformation, and phosphate P6 are bridged by two water ligands of a magnesium ion. As observed with type 1 distances, cations in the two magnesium-containing forms often occupy similar positions on the DNA surface (e.g. bridging of P9 and P10). In several cases, two or more different bridges between phosphate groups exist in the mixed spermine/magnesium and magnesium forms. Conversly, only one water or ion bridge per guanosine or cytosine phosphate pair exists in the pure-spermine form. From Table 2, it is apparent that distances between phosphate oxygen atoms and water molecules which bridge magnesium ions and phosphate groups are considerably shorter than distances between phosphate oxygen atoms and uncoordinated water molecules. Contacts between water molecules and phosphate oxygen atoms shorter than 2·5 Å always

go along with a coordination of the water molecule to a magnesium ion. On the other hand, positively charged amino and imino nitrogens of spermine molecules found in the three structures bind to the phosphate oxygen atoms directly, without an intervening water molecule.

Type 3 distances are much longer than 5′-3′ phosphate distances of types 1 and 2. In the mixed spermine/magnesium form only the two shortest type 3 distances are bridged by two water molecules. The only existing water bridge in the magnesium form, the one between phosphates P8 and P10, indicates, that an hydrated magnesium ion can span a gap of almost 8 Å. Changes in orientation and ionic environment in the pure-spermine form are accompanied by considerable conformational alterations of the left-handed duplex (Egli *et al.*, 1991; Bancroft *et al.*, 1993). This results in type 3 distances which are about 1 Å shorter on average than those for duplexes in the mixed spermine/magnesium and magnesium forms (Table 2). With two exceptions 5′-3′ phosphate groups at GpC steps are therefore bridged by water molecules in that form. It was mentioned before that a Z_{II} conformation of a phosphate renders formation of water bridges between 5′-3′ phosphate groups of guanosine and cytidine residues impossible. However, close inspection of Table 2 reveals that the shortest intra-strand type 3 distances occur between phosphate groups which enclose a phosphate adopting a Z_{II} conformation. In both the mixed spermine/magnesium (P4, P6) and the pure-spermine form (P8, P10), such phosphate groups are bridged by two water molecules.

(d) *Inter-strand water structure between anionic phosphate groups*

Similar to the classification of intra-strand contacts between phosphate groups, one can differentiate between various types of inter-strand contacts between phosphate groups within columns of stacked hexamer duplexes. Two types of contacts across the minor groove lie within a distance range which can be possibly bridged by water molecules or ions. We will refer to these as distance types 4 (Figure 1A, continuous orange line connecting P2 and P8#) and 5 (Figure 1A, broken orange line connecting P2 and P10#), which correspond to the closest transversal and longitudinal contacts between phosphate groups across the groove, respectively. Distances and water structure for the two inter-strand types are listed in Table 3.

The closest inter-strand phosphate distances (transversal, type 4) are considerably larger than the closest intra-strand phosphate distances (type 1 and 2), but still smaller than the intra-strand type 3 distances. Three inter-strand distances of type 4 are found in the hexamer structures, one of them involving two stacked helices (P2-P8#). In the mixed spermine/magnesium form, two of the phosphate pairs separated by type 4 distances are bridged by two water molecules. Similarly, in the magnesium form two solvent bridges exist between phosphates P6 and P10, each consisting of two water molecules coordinated to two different magnesium ions. However, the longitudinal inter-strand distances (type 5) in both magnesium ion-containing forms are too large to allow any simple ordered water structure.

Due to the reduced helical rise per base-pair in the pure-spermine form, type 5 distances are considerably shorter than the corresponding distances in the magnesium ion-containing forms (Table 3). Consequently, phosphate pairs P2-P10# and P4-P8# are each bridged by two water molecules. Only one type 4 distance is bridged in the pure-spermine form (P6-P10). Although the two other phosphate pairs are separated by type 4 distances which are short enough to be bridged by water molecules, no defined water structure exists at these sites. The spermine molecule which binds to the minor groove most likely disrupts the formation of water bridges which connect phosphates transversally across the minor groove.

Compared to the hydration of the bases in the groove, phosphate hydration patterns appear less regular at first. However, a careful analysis of the variation of the inter-phosphate distances reveals that a single water bridge is always present when the distance between the closest phosphate oxygen atoms is less than 4·7 Å, irrespective from the position within the alternating backbone (P3-P4, P5-P6, P10-P11, P11-P12, see Table 2). In the only exception, where a larger gap is bridged by a single water molecule (P2-P3 in the pure-spermine form, 4·95 Å), the distance between one of the phosphate groups and the water molecule is rather long. Solvent bridges involving two water molecules with reasonable geometries are only found between phosphate oxygen atoms separated by distances of up to about 6·5 Å, while magnesium hexahydrate complexes can fill a gap of up to almost 8 Å (Figure 7). The increased binding capacity of the water molecules within the first hydration shell of the magnesium ion is caused by the electrostatic polarization and is apparent from the shorter hydrogen bond distances between such water molecules and the phosphate oxygen (as low as 2·4 Å). Thus, phosphate hydration is systematic in a sense that it reflects the distance relations of the *Z*-DNA duplex within and between the two backbones.

(e) *Thermal motion*

X-ray crystallographic analyses provide information on the motion of molecules and ions in the crystal. Like the atomic coordinates, the individual *B*-factors of atoms are more or less tightly restrained during crystallographic refinement of macromolecular structures. To compare the thermal motion of specific portions of the DNA among the three forms of the *Z*-DNA hexamer, the *B*-factors of bases, deoxyriboses and phosphates were averaged for each nucleotide in the three duplexes and plotted separately (Figure 8). Phosphate groups

Table 3

Inter-strand water structure between phosphate groups

Residues	P···P distance	PO···OP distance	Water structure (maximum of 2 bridging water molecules or ion atoms)
A. *Mixed spermine/magnesium form*			
Type 4 distances			
P2···P8†	8·53 Å	6·26 Å	**P-O**···3·01 Å···$\mathbf{W}^{19,A^2}_{120}$···2·88 Å···$\mathbf{W}^{7,A^2}_{118}$···2·76 Å···**O-P**
			P-O···2·72 Å···$\mathbf{W}^{12,A^2}_{92}$···3·34 Å···$\mathbf{W}^{31,A^2}_{117}$···2·91 Å···**O-P**
P4···P12	8·63 Å	7·29 Å	None
P6···P10	8·88 Å	6·95 Å	**P-O**···3·12 Å···$\mathbf{W}^{39,A^2}_{144}$···3·13 Å···$\mathbf{W}^{16,A^2}_{103}$···2·74 Å···**O-P**
			P-O···2·72 Å···$\mathbf{W}^{13,A^2}_{104}$···2·88 Å···$\mathbf{W}^{20,A^2}_{142}$···3·09 Å···**O-P**
Mean	8·68 Å	6·83 Å	
(σ)	(0·15 Å)	(0·43 Å)	
Type 5 distances			
P2···P10†	10·56 Å	8·48 Å	None
P4···P8†	11·12 Å	9·19 Å	None
P6···P12	11·50 Å	9·59 Å	None
Mean	11·06 Å	9·09 Å	
(σ)	(0·39 Å)	(0·46 Å)	
B. *Magnesium form*			
Type 4 distances			
P2···P8†	8·56 Å	6·59 Å	None
P4···P12	8·79 Å	7·08 Å	None
P6···P10	8·57 Å	6·72 Å	**P-O**···3·26 Å···$\mathbf{MgW}^{21,A^2}_{91}$···2·97 Å···$\mathbf{MgW}^{20,A^2}_{157}$···2·44 Å···**O-P**
			P-O···3·10 Å···$\mathbf{MgW}^{20,A^2}_{92}$···3·09 Å···$\mathbf{MgW}^{20,A^2}_{134}$···2·44 Å···**O-P**
Mean	8·64 Å	6·80 Å	
(σ)	(0·11 Å)	(0·21 Å)	
Type 5 distances			
P2···P10†	10·91 Å	8·91 Å	None
P4···P8†	11·59 Å	9·69 Å	None
P6···P12	11·00 Å	9·12 Å	None
Mean	11·17 Å	9·24 Å	
(σ)	(0·30 Å)	(0·33 Å)	
C. *Pure spermine form*			
Type 4 distances			
P2···P8†	8·51 Å	6·18 Å	None
P4···P12	8·36 Å	6·70 Å	None
P6···P10	8·38 Å	6·43 Å	**P-O**···3·32 Å···$\mathbf{W}^{30,A^2}_{108}$···3·08 Å···$\mathbf{SpmN14}^{35,A^2}_{131}$···2·64 Å···**O-P**
Mean	8·42 Å	6·44 Å	
(σ)	(0·07 Å)	(0·21 Å)	
Type 5 distances			
P2···P10†	8·57 Å	7·22 Å	**P-O**···2·95 Å···$\mathbf{W}^{24,A^2}_{107}$···3·06 Å···$\mathbf{W}^{33,A^2}_{117}$···2·68 Å···**O-P**
P4···P8†	10·01 Å	7·79 Å	**P-O**···2·74 Å···$\mathbf{W}^{31,A^2}_{168}$···3·25 Å···$\mathbf{W}^{34,A^2}_{132}$···2·54 Å···**O-P**
P6···P12	10·38 Å	8·08 Å	None
Mean	9·65 Å	7·70 Å	
(σ)	(0·78 Å)	(0·36 Å)	

The Table lists selected inter-strand distances between phosphorus atoms and the shortest of the 4 possible P-O···O-P distances, as well as distances between phosphate oxygen atoms and water molecules and between water molecules. Angles at the water molecules are in subscript, their isotropic temperature factors are in superscript. Symmetry-related atoms are marked (†). The distance types 4 and 5 are defined in the text.

(atoms P, O-1P, O-2P, O-3′ and O-5′) show much higher mobility than sugars and bases. Mobility of the sugars is intermediate and is still higher than that of the bases. Careful comparison of atomic group mobilities in the mixed spermine/magnesium and magnesium forms shows that the mobilities of residues follow very similar patterns in the two structures. This is a remarkable finding since, although the two structures are isomorphous, the local ionic environments of the duplexes are quite different in the two cases. From the relative mobilities particularly of the base atoms, it can be concluded that the motions of the duplex at the two ends differ considerably in both forms. It appears reasonable to attribute the lower *B*-factors of atoms in the mixed spermine/magnesium form at least partway to a somewhat more restrictive refinement, but to a bigger extent to the slightly higher resolution of the X-ray data in that form. The different orientation of the duplex in the unit cell of the pure-

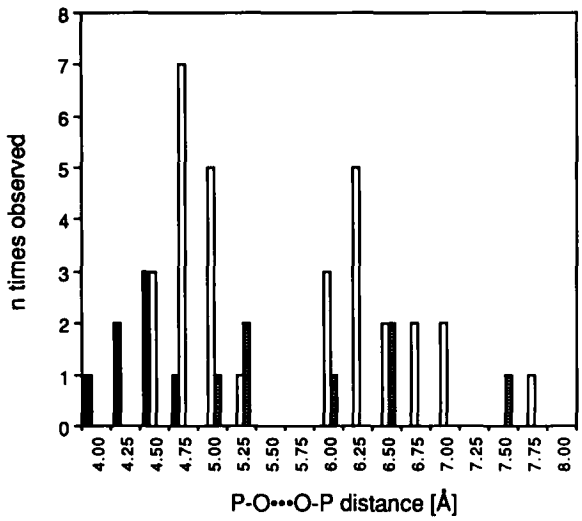

Figure 7. Histogram illustrating the relation between the type of intra and inter-strand phosphate hydration and the distances separating the phosphates in the 3 *Z*-DNA structures. The bars indicate the number of occurences of a specific type of bridging: phosphate groups bridged by a single water molecule (black), phosphate groups bridged by 2 water molecules or one water molecule and a protonated nitrogen of spermine (white), and phosphate groups bridged by 2 water molecules from the first hydration shell of a magnesium ion (hatched).

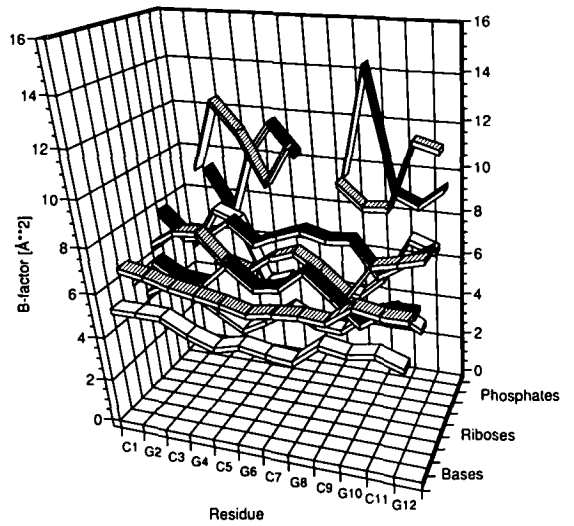

Figure 8. Averaged atomic *B*-factors of bases, riboses and phosphate groups for mixed spermine/magnesium form (open ribbons), magnesium form (hatched ribbons), and pure-spermine form (black ribbons). For the calculation of the average *B*-factors, the O-5′ and O-3′ oxygens were assigned to the phosphate groups.

spermine form goes along with characteristic changes of the relative mobilities of residues within the duplex compared to the two other forms.

In the three structures, the temperature factors of the water molecules which coordinate directly to functional groups of the bases are generally lower than those of water molecules hydrogen-bonded to phosphate groups or located in the second shell of hydration. For water molecules of the first hydration shell, the water *B*-factor and the distance between water molecule and DNA atom are weakly correlated (Figure 9). Intuitively, such a dependence seems reasonable and its existence among the first hydration shell water molecules therefore renders the determined *B*-factors physically meaningful. Water molecules coordinating to phosphate groups display a more irregular pattern and *B*-factors and distances are not correlated. A characteristic of phosphate hydration is the fact that quite a few water molecules with short contacts to phosphate oxygens possess relatively high *B*-factors. This reflects the mobility of the phosphate groups themselves.

4. Conclusions

In each of the three structures of the hexamer d(CGCGCG) discussed here, there are four highly conserved hydration motifs (the branched transversal water bridge between N-2 atoms of guanosine residues and phosphate groups is counted as one motif in this context). Two longitudinal motifs are located on the convex surface of the DNA and a third one is the spine of hydration along the minor groove. In the pure-spermine form, some water molecules of the spine of hydration are replaced or displaced by a spermine molecule. An important feature of these three motifs is the bridging of base positions from alternative strands. This is a unique feature of *Z*-DNA, and the water structures surrounding *A* and *B*-DNA rather involve bridging water molecules within strands than across the grooves. The specific arrangement of water molecules around *Z*-DNA is the result of the particular alignments of the cytosine O-2 keto groups in the minor groove and of the cytosine N-4 and guanine O-6 groups in the major groove, which are roughly parallel to the helical axis. This particular geometry derives from the position of the helical axis in the minor groove close to cytosine O-2 positions, as well as from the *Z*-DNA characteristic

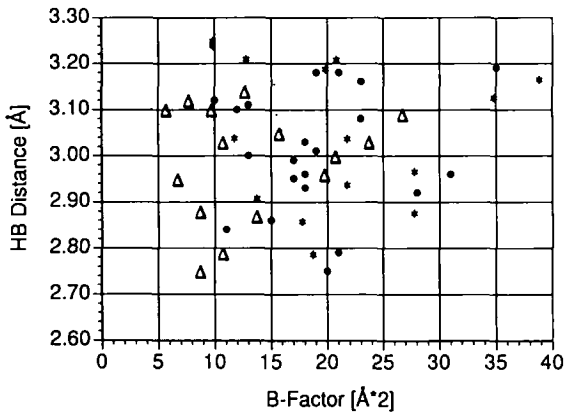

Figure 9. Correlation of water molecule *B*-factor and hydrogen bonding distance with water molecules bound to the DNA bases for mixed spermine/magnesium form (open triangles), magnesium form (filled circles), and pure-spermine form (asterisks).

conformational alternation between a small twist and a large shear in the CpG step and a large twist and a small shear in the GpC step. Together with the transversal water structure between guanosine N-2 atoms and phosphate groups in the minor groove, two hydrogen bonds to bridging water molecules per base-pair are thus formed both on the convex surface and in the minor groove. This conserved arrangement of water molecules should contribute to the increased rigidity of the *Z*-DNA helix compared to the right-handed conformations. The specific hydration may also contribute to the strong sequence dependence of the *Z*-DNA conformation.

In the three structures analyzed, the positions of many water molecules which are part of the first hydration shell are strongly conserved. Such water molecules can maintain their specific contacts to the DNA even when the local environment is altered (binding of hydrated mono- or divalent metal cations or organic polycations to the DNA), or when the DNA molecule itself assumes a different orientation in the crystallographic unit cell, and a consequently globally altered duplex environment. Whether water molecules are located on the convex surface or in the narrow, more shielded minor groove seems to be unimportant for the degree of conservation of water positions in the case of the examined *Z*-DNA hexamers. Since a specific hydration motif occurs in most or even all residues, as is the case in the three structures investigated here, there is a strong likelyhood for it to be also present, in a more dynamic way, in solution. This conclusion is not restricted to left-handed *Z*-DNA and may be a general principle with conserved hydration motifs located around DNA. Recent NMR experiments suggest that the spine of hydration in the minor groove of the *B*-DNA dodecamer d(CGCGAATTCGCG) remains intact in solution (Kubinec & Wemmer, 1992; Liepinsh, *et al.*, 1992).

From the hydration patterns around bases and phosphate groups in the *Z*-DNA hexamers no simple conclusion regarding the role of water in the conformational transition between right-handed *B* and left-handed *Z*-DNA can be drawn. Although some of the phosphate groups are bridged by a single water molecule, a motif where two phosphate groups are bridged by two water molecules prevails. A similar number of water molecules is therefore necessary to hydrate either the backbones of *Z*-DNA or *B*-DNA. Nevertheless, distances between phosphate groups and the number and geometrical arrangements of water molecules connecting them are intimately related in the three *Z*-DNA structures. The water structure appears to adapt itself to the distance constraints which govern the arrangements of pairs of phosphate groups. However, compared to water bridges between base nitrogen atoms and phosphate groups in the minor groove, where the cutoff distance for a single water bridge is about 6·0 Å, it is about 4·7 Å in the case of interphosphate hydration. This shorter distance can be partly attributed to the phosphate-induced polarization of the water molecules (resulting in smaller hydrogen bond angles), and partly to the intrinsically higher motion of phosphate groups compared to bases in DNA. In the three structures, the temperature factors of those water molecules which are bound to functional groups of bases are significantly lower than the ones of water molecules arranged around the phosphate groups. Thus, similar to the way the topological and functional features of the DNA are reflected by the arrangement of the first hydration shell water molecules, the dynamic properties of the DNA are also transmitted on the water molecules surrounding it.

This paper is dedicated to Professor Alexander Rich on the occasion of his 70th birthday.

References

Bancroft, D., Williams, L. D., Rich, A. & Egli, M. (1994). The low temperature crystal structure of the pure-spermine form of *Z*-DNA reveals binding of a spermine molecule in the minor groove. *Biochemistry*, in the press.

Berman, H. M. (1991). Hydration of *B*-DNA. *Curr. Opn. Struct. Biol.* **1**, 423–427.

Chen, S.-L. & Quigley, G. J. (1992). The oligonucleotide d(CpGpCpGpCpG) is a Z_I/Z_{II} hybrid at liquid nitrogen temperature. *Conf. Abstr. American Crystallographic Association 1992 Annual Meeting/Pittsburgh Diffraction Conference, 50th Annual Meeting, ACA symp ser. 2*, vol. 20, p. 103.

Chevrier, B., Dock, A. C., Hartmann, B., Leng, M., Moras, D., Thuong, M. T. & Westhof, E. (1986). Solvation of the left-handed hexamer d(5BrC-G-5BrC-G-5BrC-G) in crystals grown at two temperatures. *J. Mol. Biol.* **188**, 707–719.

Chuprina, V. P., Heinemann, U., Nurislamov, A. A., Zielenkiewicz, P., Dickerson, R. E. & Saenger, W. (1991). Molecular dynamics simulation of the hydration shell of a *B*-DNA decamer reveals two main types of minor-groove hydration depending on groove width. *Proc. Nat. Acad. Sci., U.S.A.* **88**, 593–597.

Cruse, W. B. T., Salisbury, S. A., Brown, T., Cosstick, R., Eckstein, F. & Kennard, O. (1986). Chiral phosphorothioate analogues of *B*-DNA. The crystal structure of Rp-d[Gp(S)CpGp(S)CpGp(S)C]. *J. Mol. Biol.* **192**, 891–905.

Drew, H. R. & Dickerson, R. E. (1981). Structure of a *B*-DNA Dodecamer. III. Geometry of hydration. *J. Mol. Biol.* **151**, 535–556.

Egli, M., Williams, L. D., Gao, Q. & Rich, A. (1991). Structure of the pure-spermine form of *Z*-DNA (magnesium free) at 1·Å resolution. *Biochemistry*, **30**, 11388–11402.

Eisenhaber, F., Mannik, J. H. & Tumanyan, V. G. (1990*a*). Structural principles of *B*-DNA grooves hydration in fibres as revealed by Monte Carlo simulations and X-ray diffraction. *Biopolymers*, **29**, 1453–1464.

Eisenhaber, F., Tumanyan, V. G. & Abagyan, R. A. (1990*b*). Structure of the hydration shells of oligo(dA-dT), oligo(dA-dT) and oligo(dA), oligo(dT) tracts in *B*-type conformation on the basis of Monte Carlo calculations. *Biopolymers*, **30**, 563–581.

Eisenstein, M., Frolow, F., Shakked, Z. & Rabinovich, D. (1990). The structure and hydration of the *A*-DNA fragment d(GGGTACCC) at room temperature and low temperature. *Nucl. Acids Res.* **18**, 3185–3194.

Finney, J. L., Goodfellow, J. M., Howell, P. L. & Vovelle, F. (1985). Computer simulation of aqueous biomolecular systems. *J. Biomol. Struct. Dynam.* **3**, 599–622.

Gessner, R. V., Quigley, G. J., Wang, A. H.-J., van der Marel, G. A., van Boom, J. H. & Rich, A. (1985). Structural basis for stabilization of *Z*-DNA by cobalt hexammine and magnesium cations. *Biochemistry*, **24**, 237–240.

Gessner, R. V., Frederick, C. A., Quigley, G. J., Rich, A. & Wang, A. H.-J. (1989). The molecular structure of the left-handed *Z*-DNA double helix at 1·0 Å atomic resolution. *J. Biol. Chem.* **264**, 7921–7935.

Harmouchi, M., Albiser, G. & Premilat, S. (1990). Changes of hydration during conformational transitions of DNA. *Eur. Biophys. J.* **19**, 87–92.

Hendrickson, W. A. & Konnert, J. H. (1981). Stereochemically restrained crystallographic least-squares refinement of macromolecule structures. *Biomolecular Structure, Conformation, Function and Evolution* (Srinivasan, R., ed.), pp. 43–57, Pergamon, Oxford.

Kagawa, T. F., Stoddard, D., Zhou, G. & Ho, P. S. (1989). Quantitative analysis of DNA secondary structure from solvent accessible surfaces: the *B*-DNA to *Z*-DNA transition as a model. *Biochemistry*, **28**, 6642–6651.

Kennard, O., Cruse, W. B. T., Nachman, J., Prange, T., Shakked, Z. & Rabinovich, D. (1986). Ordered water structure in an *A*-DNA octamer at 1·7 Å resolution. *J. Biomol. Struct. Dyn.* **3**, 623–647.

Kopka, M. L., Fratini, A. V., Drew, H. R. & Dickerson, R. E. (1983). Ordered water structure around a *B*-DNA dodecamer. A quantitative study. *J. Mol. Biol.* **163**, 129–146.

Kubinec, M. G. & Wemmer, D. E. (1992). NMR evidence for DNA bound water in solution. *J. Amer. Chem. Soc.* **114**, 8739–8740.

Liepinsh, E., Otting, G. & Wüthrich, K. (1992). NMR observation of individual molecules of hydration water bound to DNA duplexes: direct evidence for a spine of hydration water present in aqueous solution. *Nucl. Acids Res.* **20**, 6549–6553.

Privé, G. G., Heinemann, U., Chandrasegaran, L.-S. K., Kopka, M. L. & Dickerson, R. E. (1987). Helix geometry, hydration, and G·A mismatch in a *B*-DNA decamer. *Science*, **238**, 498–504.

Quigley, G. J., Teeter, M. M. & Rich, A. (1978). Structural analysis of spermine and magnesium ion binding to yeast phenylalanine transfer RNA. *Proc. Nat. Acad. Sci., U.S.A.* **75**, 64–68.

Saenger, W. (1987). Structure and dynamics of water surrounding biomolecules. *Annu. Rev. Biophys. Biophys. Chem.* **16**, 93–114.

Saenger, W., Hunter, W. N. & Kennard, O. (1986). DNA conformation is determined by economics in the hydration of phosphate groups. *Nature (London)*, **324**, 385–388.

Schneider, B., Cohen, D. & Berman, H. M. (1992*a*). Hydration of DNA bases: analysis of crystallographic data. *Biopolymers*, **32**, 725–750.

Schneider, B., Ginell, S. L., Jones, R., Gaffney, B. & Berman, H. M. (1992*b*). Crystal and molecular structure of a DNA fragment containing a 2-aminoadenine modification: the relationship between conformation, packing, and hydration in *Z*-DNA hexamers. *Biochemistry*, **31**, 9622–9628.

Shakked, Z., Guerstein-Guzikevich, G., Eisenstein, M., Frolow, F. & Rabinovich, D. (1989). The conformation of the DNA double helix in the crystal is dependent on its environment. *Nature (London)*, **342**, 456–460.

Subramanian, P. S. & Beveridge, D. L. (1993). A Monte-Carlo simulation study of the aqueous hydration of d(CGCGCG) in *Z*-form. *Theoret. Chim. Acta*, **85**, 3–15.

Subramanian, P. S., Ravishanker, G. & Beveridge, D. L. (1988). Theoretical considerations on the 'spine of hydration' in the minor groove of d(CGCGAATTCGCG)-d(CGCGAATTCGCG): Monte Carlo computer simulation. *Proc. Nat. Acad. Sci., U.S.A.* **85**, 1836–1840.

Subramanian, P. S., Swaminathan, S. & Beveridge, D. L. (1990). Theoretical account of the 'spine of hydration' in the minor groove of duplex d(CGCGAATTCGCG). *J. Biomol. Struct. Dynam.* **7**, 1161–1165.

Wang, A. H.-J., Quigley, G. J., Kolpak, F. J., Crawford, J. L., van Boom, J. H., van der Marel, G. A. & Rich, A. (1979). Molecular structure of a left-handed double helical DNA fragment at atomic resolution. *Nature (London)*, **282**, 680–686.

Wang, A. H.-J., Quigley, G. J., Kolpak, F. J., van der Marel, G. A., van Boom, J. H. & Rich, A. (1981). Left-handed double helical DNA: variations in the backbone conformation. *Science*, **211**, 171–176.

Westhof, E. (1987). Hydration of oligonucleotides in crystals. *Int. J. Biol. Macromol.* **9**, 186–192.

Westhof, E. (1988). Water: an integral part of nucleic acid structure. *Annu. Rev. Biophys. Biophys. Chem.* **17**, 125–144.

Zhou, G. W. & Ho, P. S. (1990). Stabilization of *Z*-DNA by demethylation of thymine bases: 1·3 Å crystal structure of d(m^{5}CGUAm^{5}CG). *Biochemistry*, **29**, 7229–7236.

Edited by B. W. Matthews

(Received 21 June 1993; accepted 26 November 1993)